DOXORUBICIN PARADOXICALLY PROTECTS CARDIOMYOCYTES AGAINST IRON-MEDIATED TOXICITY: ROLE OF REACTIVE OXYGEN SPECIES AND FERRITIN

[‡]Gianfranca Corna, [◊]Paolo Santambrogio, ¶Giorgio Minotti and [‡§]Gaetano Cairo

[‡]Institute of General Pathology, Via Mangiagalli 31, 20133 Milan; [◊]Protein Engineering Unit Dibit, IRCCS H. S. Raffaele, Via Olgettina 58, 20132 Milan; ¶Department of Drug Sciences and Centro Studi sull'Invecchiamento, G. D'Annunzio University School of Medicine, Chieti, Via dei Vestini, 66013 Chieti; ITALY

Running title : Doxorubicin, cardiotoxicity, and iron

G. Corna, G. Minotti and G. Cairo contributed equally to this paper

Correspondence should be addressed to:
Gaetano Cairo,
Istituto Patologia Generale,
Università di Milano,
Via Mangiagalli 31,
20133 Milano,
Italy
Tel +39 0250315350; Fax +39 0250315338
e-mail: gaetano.cairo@unimi.it

SUMMARY

The cardiotoxicity induced by the anticancer anthracycline doxorubicin (DOX) is attributed to reactions between iron and reactive oxygen species (ROS) that lead to oxidative damage. We found that DOX forms ROS in H9c2 cardiomyocytes, as shown by dichlodihydrorofluoresceine oxidation and the expression of stress-responsive genes such as catalase or aldose reductase. DOX also increased ferritin levels in these cells, particularly the H subunit. A considerable increase in ferritin mRNA levels showed that DOX acted at transcriptional level, but an additional potential mechanism was identified as the down-regulation of iron regulatory protein-2, post-transcriptional inhibitor of ferritin synthesis. Pretreatment with DOX protected H9c2 cells against the damage induced by subsequent exposure to ferric ammonium citrate, and experiments with ^{55}Fe revealed that the protection was due to the deposition of iron in ferritin. Cytoprotection was also observed when DOX was replaced by glucose/glucose oxidase, a source of H_2O_2, thus suggesting that DOX increases ferritin synthesis through the action of ROS. This concept was supported by three more lines of evidence: i) DOX-induced ferritin synthesis was blocked by N-acetylcysteine, a scavenger of ROS; ii) mitoxantrone, a ROS-forming analogue, similarly induced ferritin expression and protected the cells against iron toxicity; iii) 5-iminodaunorubicin, an analogue lacking ROS-forming activity did not induce ferritin synthesis or protect the cells against iron toxicity. These results characterise a paradoxically beneficial link between anthracycline-derived ROS, increased ferritin synthesis and resistance to iron-mediated damage. The role of iron and ROS in anthracycline-induced cardiotoxicity may therefore be more complex than previously believed.

Key words : Doxorubicin; cardiotoxicity; iron, reactive oxygen species; ferritin

INTRODUCTION

Doxorubicin (DOX[1]) is an anticancer anthracycline whose therapeutic efficacy is limited by the possible development of severe cardiotoxicity. It has been suggested that both iron and reactive oxygen species (ROS) mediate the cardiotoxicity induced by DOX, but the mechanisms through which iron and ROS interact and damage cardiac cells are still debated. It has long been known that one-electron redox cycling of a quinone moiety in the tetracyclic ring of DOX is accompanied by the formation of ROS-like superoxide ($O_2^{\cdot -}$) and hydrogen peroxide (H_2O_2). Iron could act by converting these ROS into more potent and damaging oxidants such as hydroxyl radicals ($^{\cdot}OH$) [1]. On the other hand, we have demonstrated that both DOX-derived ROS and other anthracycline metabolites such as the side chain secondary alcohol metabolite doxorubicinol (DOXol) may act by altering the function of the cytoplasmic iron regulatory proteins (IRP) that govern iron homeostasis by binding to iron-responsive elements (IRE) in the untranslated regions of mRNAs for transferrin receptor (TfR) and ferritin [1]. When activated, IRPs enhance TfR mRNA stability and block ferritin mRNA translation, thus favouring iron uptake over sequestration and forming a pool of iron available for metabolic use. Conversely, the down-regulation of IRP activity allows ferritin synthesis to proceed and reduces TfR expression, thus preventing an accumulation of potentially toxic excess iron [2,3]. Studies of cell-free systems and isolated cardiomyocytes have shown that the secondary alcohol moiety of DOXol oxidises with the [4Fe-4S] cluster of cytoplasmic aconitase, a process that regenerates DOX while also inducing cluster disassembly and the consequent change of aconitase into active IRP-1 [4,5]. Subsequent interactions of DOX with cluster-released iron

[1] DOX = doxorubicin; ROS = reactive oxygen species; IRE = iron responsive elements; IRP = iron regulatory proteins; TfR = transferrin receptor; Ft = ferritin; FAC = ferric ammonium citrate; Fe= iron; ELISA= enzyme-linked immunosorbent assay.

form an anthracycline-iron complex that irreversibly oxidises the newly formed IRP-1, thus giving a "null" protein that lacks RNA-binding activity even in the presence of a reducing agent such as 2-mercaptoethanol [4,5]. Quinone-derived ROS synergise with anthracycline-iron complexes in promoting the oxidation of IRP-1 to a null protein [5]; at the same time, ROS play an independent role in promoting oxidative modifications in a clusterless IRP-2, thus priming it to ubiquitination and proteasome-mediated degradation [5,6]. DOX therefore seems to alter the normal functioning of both IRPs through a sequential action of DOXol and ROS on aconitase/IRP-1 or an independent action of ROS on IRP-2. These mechanisms may act as important links between anthracyclines and ROS and iron-mediated toxicity. It is worth noting that a number of chemical and physical or biological sources of ROS have been shown to induce transcriptional activation of ferritin synthesis, an effect that could be of benefit if the ferritin sequestered iron before it reacted with ROS to generate potent cell oxidants [7]. Whether this occurs in cells exposed to DOX-derived ROS has not been formally established.

In order to improve our understanding of the role of iron and ROS in anthracycline-induced cardiotoxicity, and given the central role that ferritin may play, we examined the expression of ferritin and its influence on iron-mediated toxicity in H9c2 rat cardiomyocytes exposed to DOX.

EXPERIMENTAL PROCEDURES

Cell culture

The H9c2 embryonic rat heart-derived cell line was obtained from The American Type Culture Collection (CRL 1446), grown at 37°C in 5% CO_2 in Dulbecco-modified MEM adjusted to contain 4 mM glutamine, 1.5 g/l sodium bicarbonate, 4.5 g/l glucose, 1mM sodium piruvate, 100 U/ml penicillin, 0.1 ng/ml streptomycin, and supplemented with 10% heat-inactivated fetal calf serum. Subconfluent cells were treated for 24 hours with various concentrations of DOX, 5-iminodaunorubicin (5-i-DNR) (Pharmacia, Milan, Italy) or mitoxantrone (Mitox) (Sigma, Milan, Italy, or incubated for various periods of time with 5 milliunits of glucose oxidase (Sigma, Milan, Italy) in the presence of 25 mM glucose in complete growth medium. In some experiments, 10 mM N-acetylcysteine (Sigma, Milan, Italy) was added to the culture medium two hours before DOX treatment. When appropriate, after exposure to anthracyclines or glucose oxidase, the cells were washed and treated for 16 hours with increasing concentrations of ferric ammonium citrate in complete medium. At the end of the various treatments, the medium was removed and the cells were washed with PBS, collected and homogenised as described below.

Preparation of cell lysates

The cells were homogenised in 10 mM Hepes, pH 7.6, 3 mM $MgCl_2$, 40 mM KCl, 5% glycerol, 0.2% Nonidet P 40 (Sigma, Milan, Italy) and a protease inhibitor cocktail (Sigma, Milan, Italy). After the addition of dithiothreitol to make a 1 mM final concentration, the lysate was centrifuged at 16.000 x g for five minutes at 4°C. Aliquots of the supernatant were taken for ELISA or immunoblot analysis and the determination of IRP activity.

RNA-protein gel retardation assay

The probe for the bandshift assay was transcribed from the linearised pSPT-fer plasmid containing the IRE of the human ferritin H chain [8] using T7 RNA polymerase in the presence of α-^{32}P UTP using a commercially available kit (Promega Corp., Milan, Italy). Equal amounts of protein (2 μg as determined using the Bio Rad protein assay kit) from the cell lysates were incubated with a molar

excess of an IRE probe and sequentially treated with RNase T1 and heparin as previously described [9]. After separation on 6% non-denaturing polyacrylamide gels, the RNA-protein complexes were visualised by autoradiography and quantitated by means of direct nuclear counting using an InstantImager (Packard Instruments Co, Milan, Italy).

Western blot analysis

Aliquots of the cytosolic extracts containing equal amounts of proteins were electrophoresed in acrylamide-SDS gels and electroblotted to Hybond ECL membranes (Amersham Co., Milan, Italy). After assessing transfer by means of Ponceau S staining, the membranes were saturated in 4 mM Tris-HCl, pH 7.6, 30 mM NaCl (TBS) containing 20% non-fat milk and 0.1% Tween-80, and incubated with rabbit antiserum to IRP-2 (raised against a conserved sequence in the degradation domain of IRP2, 1:100 dilution), catalase (Sigma, Milan, Italy, 1:5000 dilution), and β-actin (Sigma, Milan, Italy, 1:10000 dilution) to control equal protein loading. In order to detect ferritin, the proteins were separated on 7.5% native polyacrylamide gels and the blots were probed with a 1:1000 dilution of rabbit polyclonal antibodies raised against recombinant mouse H ferritin subunit [10]. After incubation with appropriate secondary antibodies and extensive washing with TBS containing Tween-80, the proteins were detected by means of chemiluminescence using an immunodetection kit (ECL Plus, Amersham Co., Milan, Italy) according to the manufacturer's instructions. The proteins were quantified by means of densitometric scanning of the blots making sure that all of the signals were in the linear range. All of the data were calculated by comparing the intensity of the bands within the same film exposure. The values were calculated after correction for the amount of β-actin.

Northern blot analysis

Total cellular RNA was isolated as previously described [11], and equal amounts of RNA were electrophoresed under denaturing conditions. To confirm that each lane contained equal amounts of total RNA, the ribosomal RNA content in each lane was estimated in ethidium bromide-stained gels by means of laser densitometry. The RNA was transferred to Hybond-N filters (Amersham Co.,

Milan, Italy) that were hybridised with the following ^{32}P-labelled DNA probes: rat ferritin H and L subunit cDNAs [12,13], and human aldose reductase cDNA [14]. Quantitative determination was obtained by means of direct nuclear counting using an InstantImager (Packard Instruments Co., Milan, Italy) and the values calculated after normalisation to the amount of ribosomal RNA.

Determination of ferritin subunit content

Ferritin concentrations were determined in cell lysates by means of ELISA using polyclonal antibodies raised against mouse recombinant H and L ferritin subunits, and calibrated using the corresponding recombinant homopolymers [10]. The specificity of the antibodies and the absence of cross-reactivity have been previously described [10]. The microtitre plates were coated with 1 μg of polyclonal antibody specific for mouse H or L ferritin. Soluble tissue homogenates or standard ferritins were diluted in 50 mM Na phosphate (pH 7.4), 150 mM NaCl, 0.05% (v/v) Tween-20, 1% bovine serum albumin (BSA), and added to the plates. The presence of ferritin was revealed by means of incubation with the same antibody labelled with horseradish peroxidase (HRP). Peroxidase activity was developed using o-phenylenediamine dihydrochloride (Sigma, Milan, Italy).

Measurement of oxidative stress

ROS production in untreated or anthracycline-treated cells was monitored using the DCFH-DA fluorescent probe (Sigma, Milan, Italy), a cell-permeable indicator of ROS [15]. DCFH-DA is activated by cellular esterases, and then the DCFH is converted by H_2O_2 and peroxidases to the DFC fluorescent derivate. After washing with PBS, the cells were loaded with DCFH-DA (20 μM) for 20 minutes at 37°C, thoroughly washed, trypsinised and resuspended in PBS. Fluorescence intensity was measured by means of FACScan flow cytometry on the FLH-1 channel.

MTT assay

H9c2 cells were seeded in quadruplicate in 24-well plates, and then left untreated or treated with DOX or DOX analogues for 24 hours. They were subsequently exposed to increasing amounts of ferric ammonium citrate (FAC) (Sigma, Milan, Italy) for 16 hours. At the end of the treatments, cell

viability was measured using thiazolyl blue (MTT, Sigma, Milan, Italy) as an indicator of mitochondrial function [16]. Briefly, 50 µl of MTT solution (5 mg/ml) were added to each well with 450 µl of medium. After incubation at 37°C for 2-3 hours, formazan crystals were dissolved by adding 500 µl of the MTT solubilisation solution and thorough pipetting up and down. Absorbance was read at 570 nm, and the background absorbance at 690 nm was subtracted.

Analysis of ^{55}Fe-labelled ferritin

H9c2 cells were incubated in the absence or presence of anthracyclines for 24 hours at 37°C in serum-free Dulbecco-modified MEM plus 0.5% bovine serum albumin added with 2 µCi/ml [^{55}Fe] ferric iron citrate (≅ 2 µM iron), which was prepared by mixing $^{55}FeCl_3$ (NEN Life Science Products, Inc. Florence, Italy) with citric acid in a 1:2 molar ratio. At the end of the incubation period, the medium was removed, and the cells were washed three times with cold PBS and homogenised in the same lysis buffer as that used for the immunoblot analysis (see above). An aliquot was taken for protein determination and another was mixed with Ultima Gold (Packard Instr. Co., Milan, Italy) in order to measure the amount of cellular ^{55}Fe by means of liquid scintillation counting. In order to evaluate ^{55}Fe incorporation into ferritin, the lysates were centrifuged, and equal amounts of proteins from the supernatants were analysed by means of the non-denaturing PAGE system used for the immunoblotting, followed by Coomassie Blue staining (to assess equal protein loading), autoradiography and IstantImager counting. The ferritin band was identified by comigration with recombinant mouse H ferritin

RESULTS

DOX induces ferritin expression

We measured ferritin levels in H9c2 cardiomyocytes exposed for 24 hours to 5-10 μM DOX, concentrations reproducing the plasma peak reached by standard infusions in patients [17]. Western blot analyses performed using an antibody against the H subunit showed that DOX increased the amount of ferritin (Fig. 1A). The antibodies against the murine ferritin subunits were also used in an ELISA to quantify the increase in ferritin and ascertain whether DOX enhanced the levels of the H and/or L subunits. Figure 1B shows that both ferritin subunits were increased by DOX, although there was a preferential induction (2.5-3 fold) of the H chain. The increase in the H subunits in the cells treated with 10 μM DOX was similar to that determined in cells exposed to iron, but the latter showed more evident accumulation of the L subunit.

Mechanisms of ferritin induction

Figure 2A shows that the IRP-1 activity measured using a bandshift assay increased in cells treated with 5 μM DOX. This result is consistent with the metabolisation of DOX to DOXol, and the ability of the latter to induce the complete disassembly of the Fe-S clusters associated with cytoplasmic aconitase, thus making the enzyme switch to IRP-1 [5]. However, at 10 μM DOX, IRP-1 activity returned to control levels (Fig. 2A) and the same was also observed when the samples were treated with 1% 2-mercaptoethanol just before the bandshift assay (not shown). This finding was consistent with the fact that DOXol oxidised back to DOX, which then damaged IRP-1 by forming a complex with iron released from the cluster [4]. As the redox activity of DOX-Fe complexes increases with the DOX:Fe ratio [18], raising DOX from 5 to 10 μM favoured the formation of DOX-Fe complexes that redox-coupled with ROS and caused the irreversible oxidation of IRP-1 into a “null” protein [5]. In addition to altering IRP-1 activity, DOX diminished the binding activity and immunodetectable levels of IRP-2 in a concentration-dependent manner. At 5 μM DOX, IRP-2 binding activity decreased by approximately 70% (Fig. 2A), which was consistent with the 60%

decrease in immunodetectable protein (Fig. 2B). The DOX-induced reductions in IRP-2 activity and levels were therefore consistent with the concentration-dependent increase in ferritin levels. This was less evident in the case of IRP-1, whose activation or inactivation at 5 μM or 10 μM DOX should have been accompanied by respectively lower or higher ferritin levels. It therefore seems that IRP-2, but not IRP-1, is involved in modulating ferritin levels after DOX treatment. However, Figure 2C shows that DOX also increased the steady-state levels of mRNAs for the ferritin H and L subunits, with a preferential (3-fold) induction of H subunit mRNA. This suggests that ferritin levels increased not only because of translational activation linked to IRP-2 down-regulation, but also because DOX increases net ferritin mRNA levels.

ROS formation in DOX-treated cells

As an increase in the transcription of the H ferritin subunit gene has been demonstrated under conditions of oxidative stress in a variety of experimental systems [7], we investigated whether ROS were involved in mediating ferritin induction in H9c2 cells exposed to DOX. We first assessed whether DOX causes oxidative stress in H9c2 cells. As shown in Figure 3A, treatment with 5 and 10 μM DOX led to increases of respectively 2.2- and 3.1-fold in the levels of mRNA for aldose reductase, a well-known stress-responsive gene [19]. Once again, the effect was similar to that observed when treating cells with iron, a specific inducer of aldose reductase [14]. Treatment with 5 and 10 μM DOX also increased the immunodetectable levels of catalase, another well-known stress-responsive gene [20], by respectively 1.5 and 2.5 times (Fig. 3B). Measurements of the oxidation of DCFH (a widely used marker of intracellular ROS formation) showed that ROS production increased 2.5-3 times in the DOX-treated cells (Fig. 3C). Taken together, these data indicate that DOX-dependent ferritin induction occurs under conditions of increased ROS production. In order to investigate the role of oxidative stress in ferritin induction, we tested whether N-acetyl-cysteine (NAC, a known ROS scavenger) prevented ferritin accumulation. Figure 3C shows that the oxidation of DCFH is inhibited in H9c2 cells treated with NAC before the

addition of DOX. Under these conditions, DOX did not increase ferritin levels, a finding that is consistent with the role of ROS in this setting (Fig. 3D).

ROS-mediated ferritin accumulation protects against iron toxicity

The fact that ferritin has a cytoprotective effect in a number of experimental models [7] prompted us to investigate whether pre-exposure to DOX could protect H9c2 cells against the damage caused by an iron load. MTT assays showed that 16 hours' iron loading caused a dose-dependent decrease in the number of viable H9c2 cells, but pre-treatment with DOX significantly improved the resistance of cells to iron-induced cell death (Fig. 4). These results indicate that the increased ferritin levels induced by DOX as a result of ROS-dependent gene activation (and perhaps IRP-2 down-regulation) protect against iron toxicity.

To assess the role of ROS further while re-addressing the role of secondary alcohol metabolites reactive to aconitase/IRP-1, we treated the H9c2 cells with anthracycline analogues characterised by their capacity to induce the formation of ROS or secondary alcohol metabolites to a different extent in comparison with DOX. The role of ROS was probed using 5-iminodaunorubicin (5-i-DNR), an analogue that contains the side-chain carbonyl group required for alcohol metabolite formation but is less than 20% as effective as DOX in generating ROS because of the presence of an imino group in place of the quinone (Fig.5). The role of secondary alcohol metabolites was probed using mitoxantrone (Mitox), an analogue that contains the quinone but lacks a carbonyl group in its side chain (Fig. 5). The experiments were performed bearing in mind that the generation of ROS and alcohol metabolites depended not only on the intrinsic biochemical behaviour of these molecules, but also on the extent to which they entered the cardiomyocytes.

On the basis of the results of our previous pharmacokinetic studies [5], 5-i-DNR and Mitox were used at concentrations of respectively 20 and 2.5 μM, which lead to the same level of uptake in cardiomyocytes as 5 μM DOX [5]. As shown in Figure 6A, measurements of DCFH oxidation confirmed that 5-i-DNR was unable to form ROS, which were formed by Mitox but apparently to a lesser extent than by DOX (Fig. 6A), probably because Mitox is an excellent reducing substrate for

H_2O_2-activated peroxidases [21]. It is quite possible that Mitox generated greater amounts of ROS than those detected by us, but its ability to react with peroxidases eventually diminished the yields of ROS which were measured on the basis of DCHF oxidation by the same peroxidases.

Having obtained information on ROS formation, we next determined whether 5-i-DNR and Mitox increased ferritin content and protected cells from iron toxicity. ELISA experiments showed that Mitox increases cell levels of ferritin (particularly the H subunit) to an extent that is similar to the increase induced by 5 μM DOX, a finding that is consistent with its ability to reach the same cell levels as DOX and to generate ROS (Fig. 6B). On the contrary, 5-i-DNR had essentially no effect on ferritin levels, which is consistent with its ineffectiveness in producing ROS. The data concerning ROS formation and ferritin levels were mirrored by those relating to iron-mediated toxicity. Figure 6C shows that 5-i-DNR (which did not form ROS or increase ferritin levels) did not protect cardiomyocytes against the damage induced by subsequent exposure to an iron load, whereas the cells pretreated with Mitox could withstand iron toxicity in a manner that was not significantly different from that of DOX (P= 0.180), which is in line with the fact that Mitox generates ROS and increases ferritin levels. Finally, Mitox had essentially the same effects as DOX despite its inability to form a secondary alcohol metabolite, thus confirming that the changes in IRP-1 activity induced by secondary alcohol metabolites are of little importance in mediating ferritin up-regulation and the consequent protection against iron toxicity.

In order to obtain further evidence that DOX-dependent ferritin induction was mediated by ROS and protected the cells from toxic iron, cardiomyocytes were exposed to a source of ROS other than DOX before undergoing iron treatment. We used the glucose/glucose oxidase reaction, which generates a constant flux of H_2O_2. As shown in Figure 7/A-C, glucose/glucose oxidase led to the robust oxidation of DCFH, increased the levels of the L and (especially) H ferritin subunits, and protected the cardiomyocytes against the damage induced by a subsequent iron exposure.

Effect of DOX on intracellular iron distribution

To obtain more direct correlations between ferritin induction and cytoprotection, we examined the fate of the radioactive iron taken up by H9c2 cells during the course of exposure to a trace amount of ^{55}Fe in the presence or absence of DOX. Autoradiography of non-denaturing gels of soluble cell homogenates showed that ferritin accounted for the vast majority of the ^{55}Fe-labelled proteins (Fig. 8). Ferritin-associated radioactivity increased if the cells were also treated with DOX or Mitox, but was not significantly enhanced by 5-i-DNR. In comparison with the cells exposed to ^{55}Fe alone, those exposed to ^{55}Fe plus DOX or the other drugs did not show any significant increase in the total cell content of ^{55}Fe determined by means of the liquid scintillation counting of aliquots of cell homogenates (not shown). This indicates that the different abilities of DOX, Mitox and 5-i-DNR to increase the incorporation of ^{55}Fe into ferritin was not mediated by enhanced cellular iron uptake and/or reduced iron release, but reflected the different extents to which the drugs up-regulate ferritin levels.

DISCUSSION

The cardiac toxicity of DOX has been attributed to its ability to generate ROS and promote iron-catalysed oxidative damage. The results of the present study show that DOX produces ROS in H9c2 cardiomyocytes, as indicated by the increased levels of stress-responsive genes such as aldose reductase and catalase, and by direct measurements of DCFH oxidation (Fig. 3). However, our results also show that DOX up-regulates ferritin levels in cardiomyocytes, and that this offers excellent protection against the toxicity induced by subsequent iron exposure. The ferritin-inducing effect of DOX consisted of a preferential increase in the H subunits (Fig. 1), a finding that is consistent with those of previous studies showing that H ferritin increase under conditions of ROS generation [9,22,23]. The role of ROS in inducing the synthesis of H ferritin and that of the H subunits in protecting against iron toxicity were demonstrated by various lines of evidence. First, ferritin synthesis was blocked by N-acetylcysteine, a ROS scavenger (Fig. 3). Secondly, neither H ferritin synthesis nor cytoprotection against iron were observed when DOX was replaced by 5-i-DNR, an analogue lacking ROS-forming activity, whereas both were seen when DOX was replaced by Mitox, an analogue that is still capable of producing ROS (Fig. 6). Thirdly, DOX-induced cytoprotection did not correlate with any substantial change in cellular iron uptake or release, but did correlate with the facilitated sequestration of iron inside ferritin (Fig. 8). Finally, anthracycline treatment led to a concomitant increase in L-type subunits, but this was small in comparison with the increase in H-type subunits and did not correlate with the ability of the analogue to provide protection against iron: in fact, the increase in L-type subunits was similar with all three drugs (Fig. 6).

We also found that 2.5 μM Mitox and 5 μM DOX are comparably taken up by cardiomyocytes and consistently induce similar increases in H ferritin, although ROS generation seemed to be less with Mitox. This last finding may introduce a caveat if ROS are involved in mediating the anthracycline-

induced increase in ferritin anthracyclines. As mentioned above, this inconsistency may reflect the interference of Mitox with the DCFH assay for ROS, thus diminishing the apparent yield of detectable ROS. Another possibility is that the induction of H ferritin may require a threshold level of ROS formation above which ferritin synthesis continues regardless of any additional formation. Finally, it is possible that many genes may be activated by DOX and contribute to mediating protection against iron.

The protective efficacy of anthracycline pretreatment against subsequent iron loading is reminiscent of the preconditioning seen with H_2O_2, a process in which exogenous H_2O_2 or hypoxia-induced mitochondrial release of H_2O_2 protects cells against subsequent damage induced by, for example, ischemia-reperfusion [24,25]. We found that glucose oxidase (a source of H_2O_2) can replace DOX in increasing ferritin levels and protecting against iron (Fig. 7), finding that is important in two respects: i) it confirms that the effects of DOX are mediated by ROS; and ii) it indicates similarities between the protection induced by DOX and that induced by H_2O_2 preconditioning

We investigated whether ferritin synthesis was enhanced by DOX as a result of changes in IRP-1 or IRP-2 activities. Our data support the possible role of ROS-dependent IRP-2 degradation in relieving a translational block of ferritin synthesis, as shown by the comparisons of the concentration-dependent patterns of ROS formation, IRP-2 degradation and the increase in ferritin after treatment with 5 and 10 μM DOX, as well as the comparisons of the effects of DOX, Mitox and 5-i-DNR. On the contrary, neither the DOX/analogue comparisons nor the bell-shaped concentration-dependent pattern of IRP-1 activation or inactivation by 5 or 10 μM DOX seem to correlate with the pattern of enhanced ferritin synthesis (Fig. 1-3 and 6). However, we acknowledge that it is important to understand how ferritin synthesis increased after treatment with 5 μM DOX, when the degradation of IRP-2 was counteracted by the activation of IRP-1. In a previous study [26], we found that cytokine-treated macrophages underwent a similarly converse up-regulation of IRP-1 and down-regulation of IRP-2, whereas the level of ferritin synthesis increased as if the

degradation of IRP-2 somehow served the prevailing mechanisms regulating it. All of these findings may be reconciled by the fact that the IRE of ferritin mRNA are preferentially bound by IRP-2 [27]. In any case, the ability of anthracyclines to protect against iron (DOX = Mitox >> 5-i-DNR) correlates with ROS formation, IRP-2 degradation and increased ferritin synthesis [5].

IRP-2 degradation is therefore a possible determinant of increased ferritin synthesis in H9c2 cardiomyocytes, but we also found that DOX considerably increased steady-state ferritin mRNA levels. Although we did not directly demonstrate increased ferritin transcription, we suggest that such a remarkable increase reflects an action at transcriptional level mediated by the direct targeting of the 5' sequences that are conserved in the regulatory regions of H and L ferritin genes, as well as many other anti-oxidant response genes [23]. Transcriptional activation therefore seems to be a prevalent mechanism of anthracycline-induced ferritin synthesis, which is possibly further accelerated as a result of IRP-2 degradation relieving a translational block. The transcriptional activation of ferritin expression and the consequent up-regulation of steady-state mRNA levels would also be sufficient to overcome a translational block possibly caused by any transient activation of IRP-1. We are currently identifying and characterising ROS-sensitive ferritin regulatory sequences.

Other investigators have obtained similar evidence supporting the preferential accumulation of iron in ferritin after the exposure of cancer or cardiac cells to DOX; however, increased ferritin iron sequestration occurred in the absence of ferritin induction and the overall mechanism of the anthracycline/iron/ferritin interactions remained uncertain, partially because the anthracycline concentrations were often too high to be of pathophysiological relevance (e.g. 20 μM) [28]. In our study, we found that anthracycline-derived ROS were related to ferritin induction, and that increased ferritin levels were related to the ability of cardiac cells to withstand iron toxicity. Our results therefore offer the basis for a reappraisal of the role of ROS and iron in the cardiac damage induced by anthracyclines, and suggest that there may be conditions under which anthracycline-derived ROS do not exacerbate iron toxicity but actually improve cell defences against iron. This

may be the case when chemotherapy increases the plasma levels of non-transferrin-bound iron, an effect that is due to the suppression of erythropoietic activity or the leakage of iron from necrotic tumoral foci [29,30]. This iron pool may well contribute to inducing cardiotoxicity if it enters cardiomyocytes and reacts with ROS, but our results suggest that one such mechanism of toxicity may be prevented by the sequestration of iron in the ferritin shells formed by the prior redox activation of anthracyclines. This concept is supported by the fact that plasma anthracycline levels peak within minutes of drug administration [17], whereas it takes days before the peak plasma levels of non-transferrin-bound iron are reached [29]. There is therefore sufficient time for anthracylines to induce ferritin synthesis and prevent the toxicity induced by subsequent exposure of the heart to iron, a pathological condition that we have mimicked by treating isolated cardiomyocytes with anthracyclines before an iron load.

In conclusion, we have characterised a paradoxical "antioxidant" mode of action of anthracyclines, which is mediated by ferritin synthesis and leads to a long-lasting protection that persists after removal of DOX from the medium or after the decay or clearance of the drugs from biological fluids or tissues. These results raise some doubts against the widely-accepted concept of the oxidative nature of cardiotoxicity, but support the idea that antioxidants do not always protect laboratory animals against cardiotoxicity, or mitigate or delay cardiotoxicity in patients. It clearly remains to be established what the precise mechanism of cardiotoxicity is, and how it may be prevented or mitigated by the use of iron chelators such as dexrazoxane [31]. Our results raise the possibility that iron and ROS become toxic as a result of reactions that extend beyond canonical oxidative damage and, among other mechanisms, may involve alterations in the metabolic use of iron [1] or its recruitment in pro-apoptotic signals that have not yet been characterised [32].

ACKNOWLEDGEMENTS

We thank Dr. M. Locati and Dr. D. Besusso for their help with the FACS analysis, Dr. D. Barisani for the kind gift of human aldose reductase cDNA, and Dr. E. Leibold for the plasmid encoding IRP-2.

This study was supported by grants from AIRC, MURST FIRB, COFIN 2001 and 2002 to G.C. and G.M., and from the MURST Center of Excellence on Aging at the University of Chieti to G.M..

REFERENCES:

1. Minotti, G., Cairo, G., and Monti, E. (1999) *Faseb J* **13**, 199-212
2. Hentze, M. W., and Kuhn, L. C. (1996) *Proc Natl Acad Sci U S A* **93**, 8175-8182
3. Cairo, G., and Pietrangelo, A. (2000) *Biochem J* **352 Pt 2**, 241-250
4. Minotti, G., Recalcati, S., Mordente, A., Liberi, G., Calafiore, A. M., Mancuso, C., Preziosi, P., and Cairo, G. (1998) *Faseb J* **12**, 541-552
5. Minotti, G., Ronchi, R., Salvatorelli, E., Menna, P., and Cairo, G. (2001) *Cancer Res* **61**, 8422-8428
6. Iwai, K., Drake, S. K., Wehr, N. B., Weissman, A. M., LaVaute, T., Minato, N., Klausner, R. D., Levine, R. L., and Rouault, T. A. (1998) *Proc Natl Acad Sci U S A* **95**, 4924-4928
7. Torti, F. M., and Torti, S. V. (2002) *Blood* **99**, 3505-3516
8. Mullner, E. W., Neupert, B., and Kuhn, L. C. (1989) *Cell* **58**, 373-382
9. Cairo, G., Tacchini, L., Pogliaghi, G., Anzon, E., Tomasi, A., and Bernelli-Zazzera, A. (1995) *J Biol Chem* **270**, 700-703
10. Santambrogio, P., Cozzi, A., Levi, S., Rovida, E., Magni, F., Albertini, A., and Arosio, P. (2000) *Protein Expr Purif* **19**, 212-218
11. Pietrangelo, A., Rocchi, E., Casalgrandi, G., Rigo, G., Ferrari, A., Perini, M., Ventura, E., and Cairo, G. (1992) *Gastroenterology* **102**, 802-809
12. Murray, M. T., White, K., and Munro, H. N. (1987) *Proc Natl Acad Sci U S A* **84**, 7438-7442
13. Leibold, E. A., Aziz, N., Brown, A. J., and Munro, H. N. (1984) *J Biol Chem* **259**, 4327-4334
14. Barisani, D., Meneveri, R., Ginelli, E., Cassani, C., and Conte, D. (2000) *FEBS Lett* **469**, 208-212
15. Duranteau, J., Chandel, N. S., Kulisz, A., Shao, Z., and Schumacker, P. T. (1998) *J Biol Chem* **273**, 11619-11624
16. Vistica, D. T., Skehan, P., Scudiero, D., Monks, A., Pittman, A., and Boyd, M. R. (1991) *Cancer Res* **51**, 2515-2520
17. Gianni, L., Vigano, L., Locatelli, A., Capri, G., Giani, A., Tarenzi, E., and Bonadonna, G. (1997) *J Clin Oncol* **15**, 1906-1915
18. Minotti, G. (1990) *Arch Biochem Biophys* **277**, 268-276
19. Spycher, S. E., Tabataba-Vakili, S., O'Donnell, V. B., Palomba, L., and Azzi, A. (1997) *Faseb J* **11**, 181-188
20. Tacchini, L., Pogliaghi, G., Radice, L., Bernelli-Zazzera, A., and Cairo, G. (1996) *Redox Report* **2**, 273-278
21. Reszka, K. J., Matuszak, Z., and Chignell, C. F. (1997) *Chem Res Toxicol* **10**, 1325-1330
22. Tacchini, L., Recalcati, S., Bernelli-Zazzera, A., and Cairo, G. (1997) *Gastroenterology* **113**, 946-953
23. Tsuji, Y., Ayaki, H., Whitman, S. P., Morrow, C. S., Torti, S. V., and Torti, F. M. (2000) *Mol Cell Biol* **20**, 5818-5827
24. Vanden Hoek, T. L., Becker, L. B., Shao, Z., Li, C., and Schumacker, P. T. (1998) *J Biol Chem* **273**, 18092-18098
25. da Silva, M. M., Sartori, A., Belisle, E., and Kowaltowski, A. J. (2003) *Am J Physiol Heart Circ Physiol* **285**, H154-162
26. Recalcati, S., Taramelli, D., Conte, D., and Cairo, G. (1998) *Blood* **91**, 1059-1066
27. Ke, Y., Wu, J., Leibold, E. A., Walden, W. E., and Theil, E. C. (1998) *J Biol Chem* **273**, 23637-23640
28. Kwok, J. C., and Richardson, D. R. (2002) *Mol Pharmacol* **62**, 888-900
29. Bradley, S. J., Gosriwitana, I., Srichairatanakool, S., Hider, R. C., and Porter, J. B. (1997) *Br J Haematol* **99**, 337-343

30. Halliwell, B., Aruoma, O. I., Mufti, G., and Bomford, A. (1988) *FEBS Lett* **241**, 202-204
31. Myers, C. (1998) *Semin Oncol* **25**, 10-14
32. Kalyanaraman, B., Joseph, J., Kalivendi, S., Wang, S., Konorev, E., and Kotamraju, S. (2002) *Mol Cell Biochem* **234-235**, 119-124

FIGURE LEGENDS

Figure 1 Effect of DOX on ferritin content of H9c2 cells.

(A) Equal amounts of proteins (50 μg) from cells exposed for 24 hours to increasing concentrations of DOX were loaded on non-denaturing polyacrylamide gels. Ferritin was immunoblotted with an antibody against mouse H ferritin and visualised by means of chemiluminescence. The same antibody recognised mouse recombinant H ferritin (rMHF), which migrated faster due to its homopolymer composition. The gel shown is representative of four independent experiments. **(B)** Quantification of H and L ferritin subunits in cytoplasmic extracts by ELISA. H9c2 cells were treated with different doses of DOX or 30 μg/ml of ferric ammonium citrate (FAC) as a positive control. Mean values ± SD of three-five experiments. * $P<0.001$, ** $P<0.005$, *** $P<0.01$, **** $P< 0.05$ vs controls.

Figure 2 Effect of DOX on IRP binding activity, IRP-2 content and ferritin mRNA levels.

(A) Bandshift assay of IRP activity. Cytoplasmic extracts of cells exposed to increasing concentrations of DOX were incubated with an excess of a ^{32}P-labelled iron-responsive element probe; RNA-protein complexes were separated on non-denaturing 6% polyacrylamide gels and revealed by means of autoradiography. The autoradiogram is representative of three independent experiments. **(B)** Immunoblot analysis of IRP-2 content. Equal amounts of proteins (80 μg) from cytoplasmic extracts were loaded on SDS gels. IRP-2 was detected using a specific polyclonal antibody and visualised by means of chemiluminescence. The same antibody recognised histidine-tagged rat recombinant IRP-2 (rIRP-2). The blots were reprobed with an antibody against β-actin as a loading control. The gel shown is representative of three independent experiments. **(C)** Northern blot analysis of ferritin mRNAs. A filter with equal amounts of total cellular RNA, as revealed by the ethidium bromide fluorescence of rRNA, was hybridised with rat H and L ferritin cDNAs. The autoradiograms are representative of three independent experiments.

Figure 3 The induction of stress genes and antioxidant-inhibitable ferritin synthesis by DOX-derived ROS.

(A) Northern blot analysis of aldose reductase expression. A filter with equal amounts of total cellular RNA, as revealed by the ethidium bromide fluorescence of rRNA, was hybridised with a human aldose reductase probe. The autoradiogram is representative of three independent experiments. **(B)** Immunoblot analysis of catalase. Equal amounts of proteins (50 μg) from cytoplasmic extracts were loaded on SDS gels. Catalase was detected using a specific polyclonal antibody and visualised by means of chemiluminescence. The blots were reprobed with an antibody against β-actin as a loading control. The results shown are representative of three independent experiments. **(C)** Evaluation of oxidative stress. DCFH oxidation was measured by means of FACS analysis monitoring fluorescence at 522 nm. Mean values ± S.D. of three experiments * $P<0.005$, ** $P<0.01$ vs control. **(D)** Quantification of H and L ferritin subunits in cytoplasmic extracts by ELISA. H9c2 cells were treated with different doses of DOX in the presence or absence of NAC. Mean values ± SD of three experiments. * $P<0.001$, ** $P<0.005$ vs control.

Figure 4 Effect of pre-treatment with DOX on iron-mediated toxicity in H9c2 cells.

The cells were left untreated or exposed for 24 hours to 5 μM DOX. After the removal of the drug and extensive washing, the cells were challenged with increasing concentrations of ferric ammonium citrate (FAC) for 16 hours. DOX treatment alone caused the death of 30-40% of the cells. Toxicity was evaluated as the percentage of viable cells after exposure to iron, as measured by MTT assay. Mean values ± SD of three experiments.

Figure 5 Structures of DOX and the analogues used in this study.

The arrows indicate biochemically important modifications in 5-iminodaunorubicin/5-I-DNR (the replacement of a quinone by an iminogroup precludes ROS formation) or mitoxantrone/Mitox (the lack of a carbonyl group in the side chain precludes the formation of a secondary alcohol metabolite).

Figure 6 Effect of pre-treatment with DOX and DOX analogues on ROS production, ferritin content and iron-mediated toxicity in H9c2 cells.

The cells were left untreated or exposed to 5 μM DOX, 20 μM 5-i-DNR or 2.5 μM Mitox for 24 hours. **(A)** ROS were measured by means of the oxidation of DCFH as described in the legend to Figure 3. Mean values ± SD of three experiments. * P<0.005, ** P<0.01 vs control. **(B)** Quantification of H and L ferritin subunits using cytoplasmic extracts and an ELISA assay as described in the legend to Figure 1. Mean values ± SD of three experiments. * P<0.001, ** P<0.005, *** P<0.01, **** P< 0.05 vs control. N.S. not significant. **(C)** Toxicity was evaluated as the post-treatment percentage of viable cells as evaluated by MTT assay. Mean values ± SD of three experiments.

Figure 7 Effect of treatment with glucose/glucose oxidase on ROS production, ferritin content and iron-mediated toxicity in H9c2 cells.

The cells were left untreated or exposed to glucose/glucose oxidase (GOX) for the indicated times (panel A), or seven hours (panels B and C). ROS production, ferritin subunits content and cytotoxicity were evaluated as described in the legend to Figure 6. Mean values ± SD of three experiments * P<0.001, ** P<0.005, *** P<0.01.

Figure 8

Effect of exposure to DOX or DOX analogues on ferritin incorporation of ^{55}Fe.

The H9c2 cells were incubated with ^{55}Fe iron citrate in the presence or absence of 5 μM DOX, 20 μM 5-i-DNR or 2.5 μM Mitox for 24 hours, and the cell extracts were analysed by means of native PAGE. Ferritin was revealed by autoradiography and identified on the basis of the migration of purified recombinant mouse H ferritin. The autoradiogram is representative of three independent experiments.

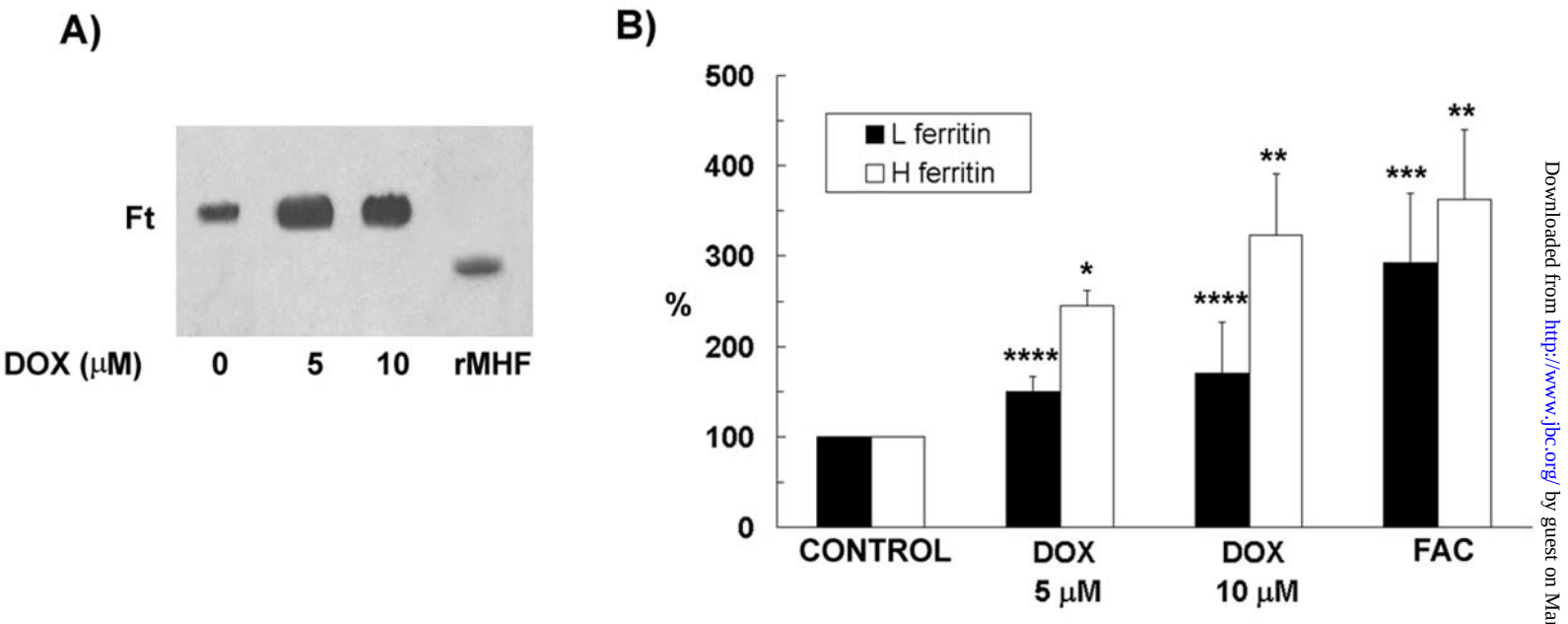

Fig. 1

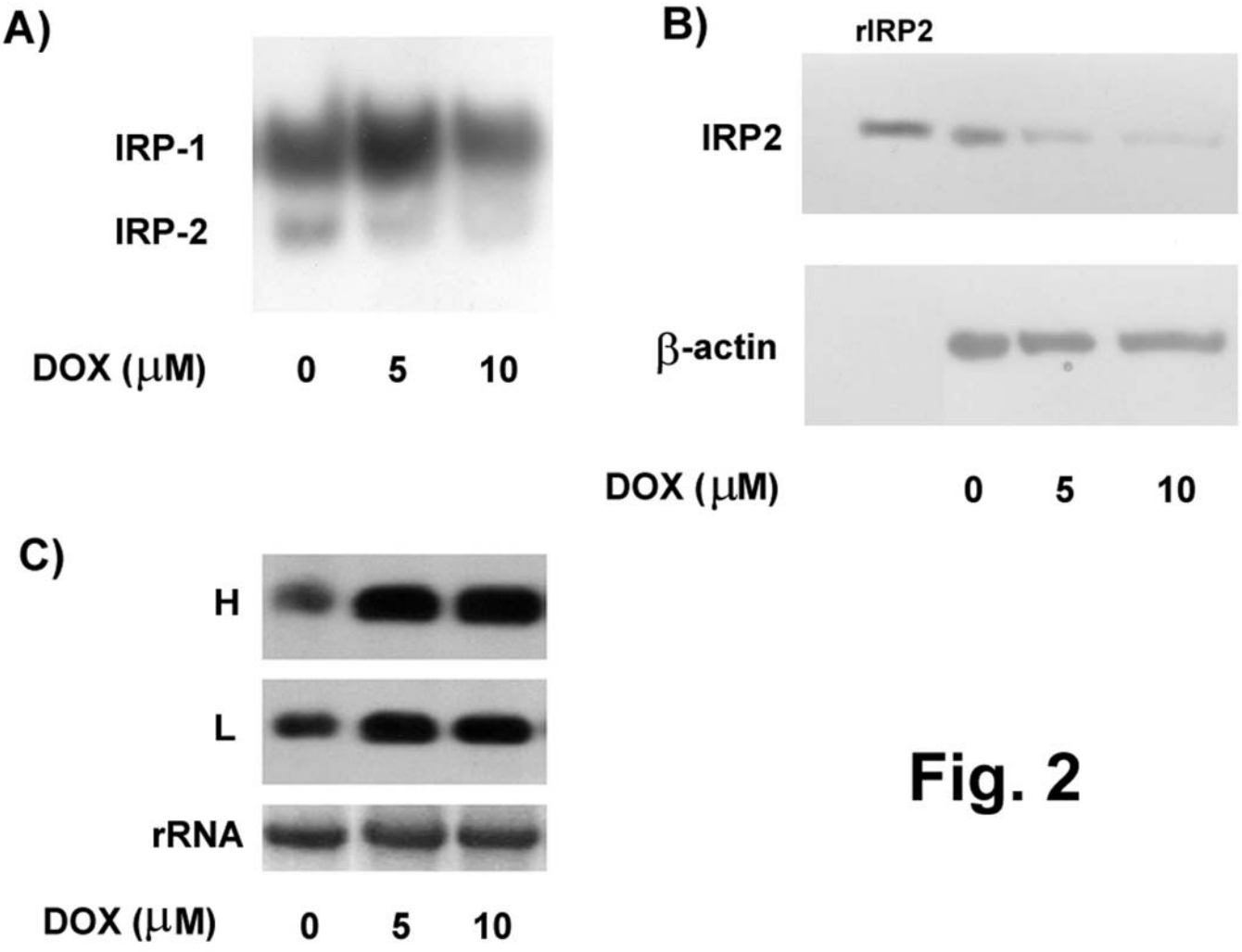

Fig. 2

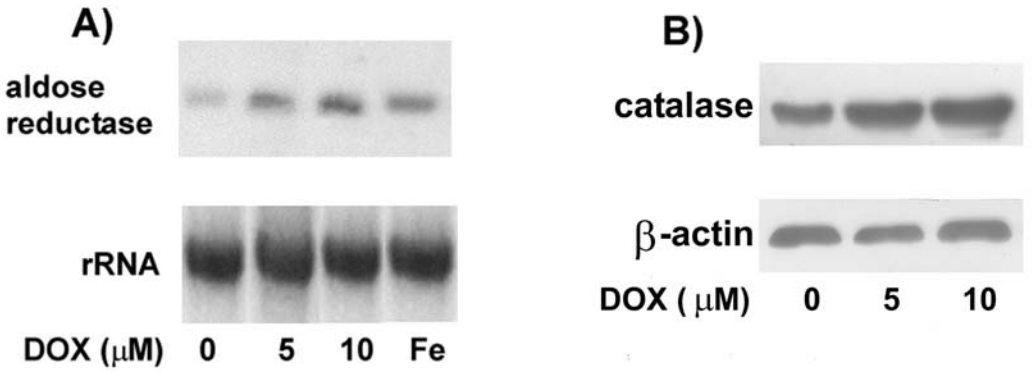

Fig. 3

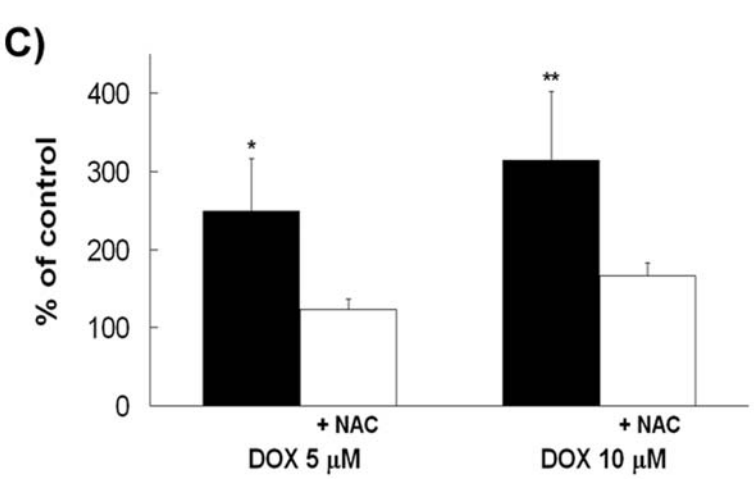

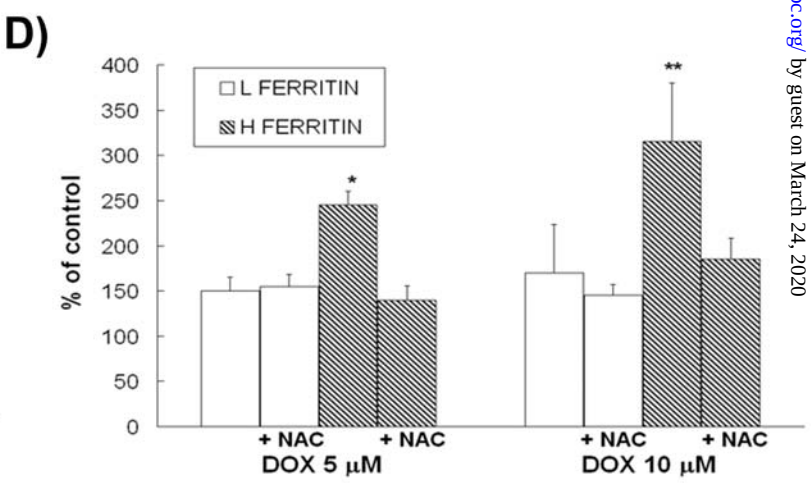

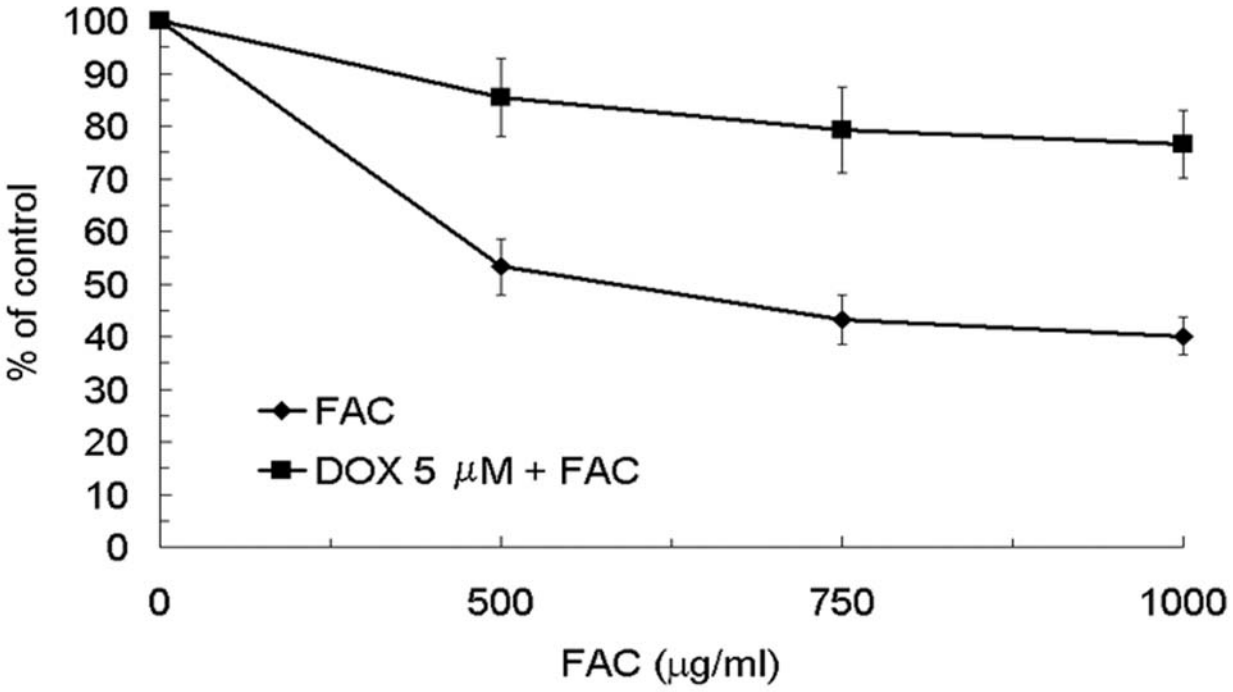

Fig. 4

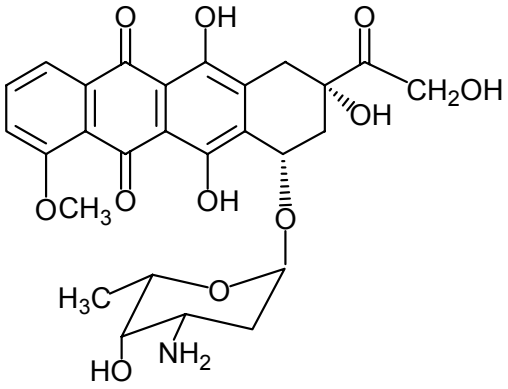

DOX

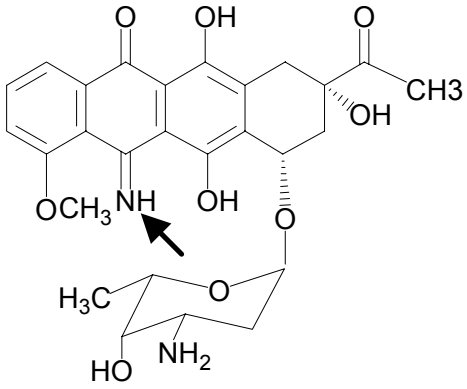

5-i-DNR

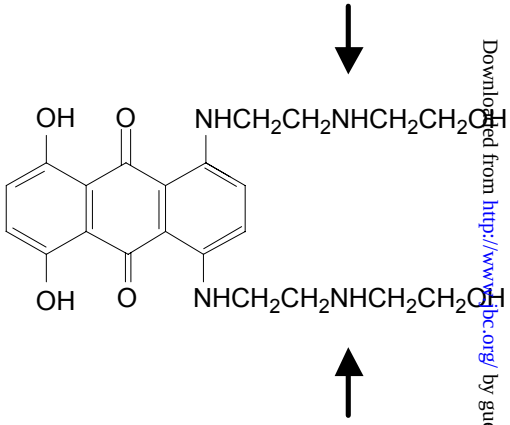

Mitox

Fig. 5

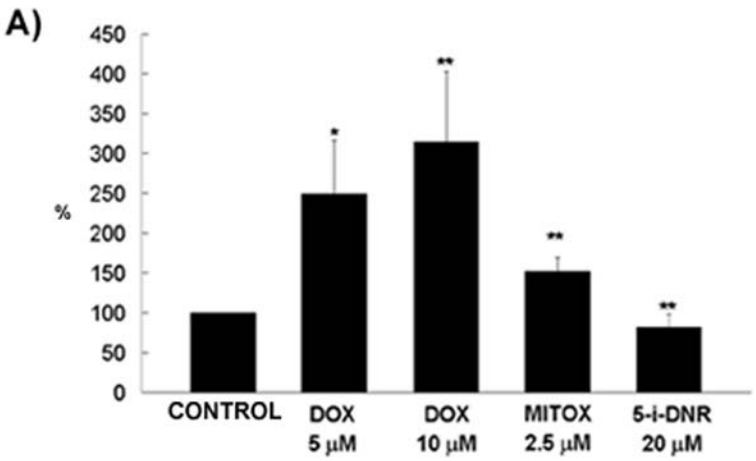

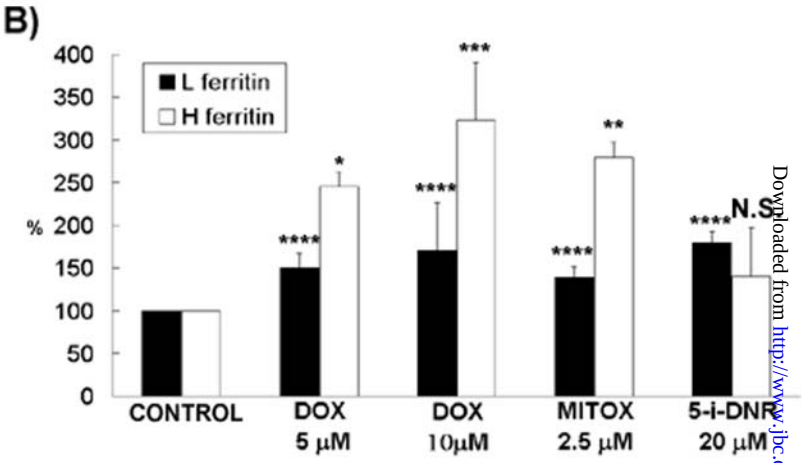

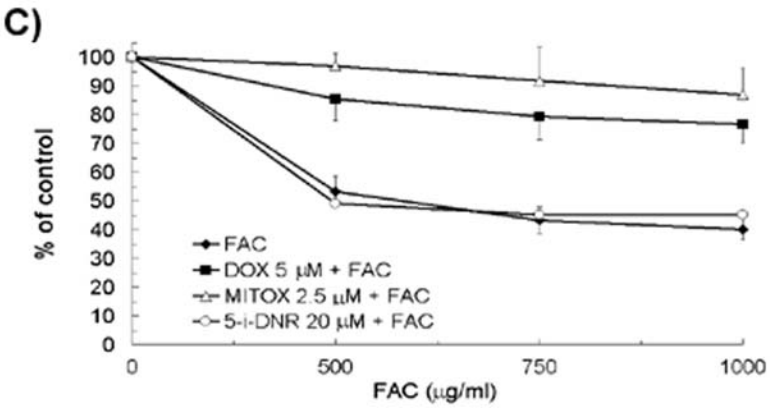

Fig. 6

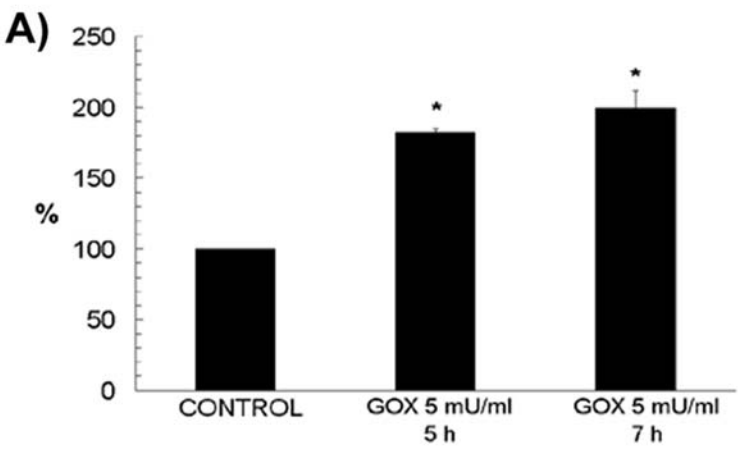

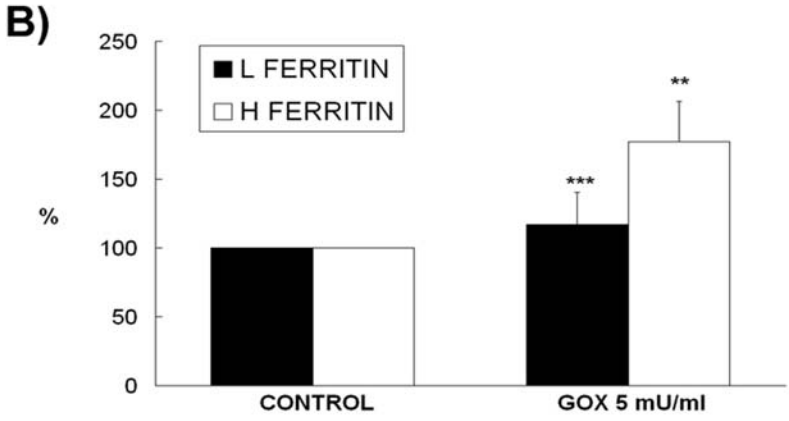

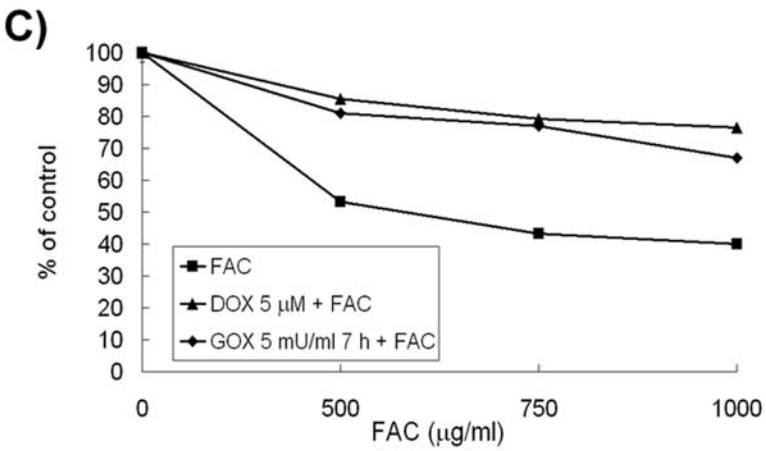

Fig. 7

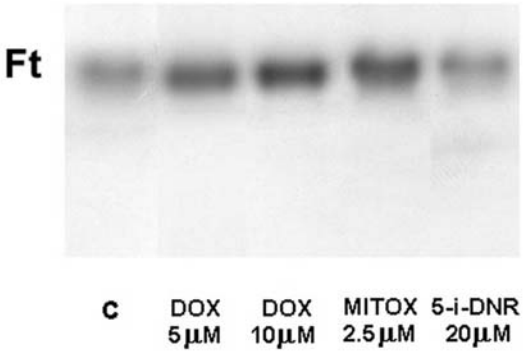

Fig. 8

Doxorubicin paradoxically protects cardiomyocytes against iron-mediated toxicity: Role of reactive oxygen species and ferritin

Gianfranca Corna, Paolo Santambrogio, Giorgio Minotti and Gaetano Cairo

J. Biol. Chem. published online January 22, 2004
